Journal of Biomechanical Science and Engineering

Vol. 2, No. 4, 2007

Stress Analysis of PS Type Knee Prostheses under Deep Flexion*

Mitsugu TODO**, Ryuji NAGAMINE*** and Shota YAMAGUCHI**

**Research Institute for Applied Mechanics, Kyushu University,
6-1 Kasuga-koen, Kasuga 816-8580, Japan
E-mail: todo@riam.kyushu-u.ac.jp
***Yoshizuka Hayashi Hospital,
7-6-29 Yoshizuka, Hakata, Fukuoka 812-0041, Japan

Abstract

3-D finite element models of two kinds of Stryker's PS type knee prostheses, Scorpio Superflex and NRG, were constructed using their CAD data with use of a nonlinear spring model and an analytical load data for deep squatting. Superflex model was formerly used in TKA, and NRG model is the latest version with a modified design of Post. Stress analysis was then performed by an explicit finite element method under continuous flexion motion from 0 to 135 degree. It was shown that only the condylar surfaces of the femoral component and the tibial insert contacted each other from 0 to 60 degree flexion for both the models, and the stress concentration in NRG was a little higher than that in Superflex. The simulation results also exhibited that severe stress concentration was generated at Post of the tibial UHMWPE insert due to Post/Cam contact. This kind of stress concentration may result in damage and failure of Post. It was shown that the design modification applied to NRG effectively reduced the stress concentration of Post.

Key words: Total Knee Arthroplasty, UHMWPE Insert, Deep Flexion, Finite Element Analysis

1. Introduction

Total knee arthroplasty, TKA, is applied to patients with severe osteoarthritis, and in general, QOL of the patients is dramatically improved after TKA. Although the function of knee prosthesis is being improved through design modification, there are still some demands for knee prosthesis such as higher durability of tibial insert and deeper flexion angle to fit Japanese life style, for example, 150 degree for kneeling on a tatami mat. It is therefore needed to understand the detail of movements of the knee after TKA, and such information should be reflected to the design of knee prosthesis. It is however very difficult to understand the detail of TKA knee motion because of its complex movements characterized as a combination of flexion, external and internal rotation and roll-back. Fatigue fracture and severe wear of tibial inserts are sometimes reported, and they are thought to be caused by the stress concentration under such complex knee motions.

PS type knee prosthesis is known to be used in a type of TKA where anterior and posterior cruciate ligaments are removed. PS type prosthesis is characterized by the existence of Post-Cam structure to stabilize the knee movement through the Post-Cam contact. In this type of prosthesis, failure and wear of Post of the tibial insert are important problems and therefore, there is a demand for understanding the stress state of the tibial insert during knee motion. Under such circumstances, three-dimensional finite element method (FEM) has been utilized to characterize the 3D stress state of knee prosthesis.

*Received 11 June, 2007 (No. 07-0250)
[DOI: 10.1299/jbse.2.237]

In the previous studies of FEM simulations of TKA, most of them were aimed to analyze stress states under walking conditions with shallow flexions [1,2-5,8], and a few attempts have been made to analyze stress state under deep flexion [9-11]. Morra and Greenwald performed a deep flexion analysis of TKA, however, their work was limited to a certain deep flexion angle under simple loading condition [9]. On the contrary, the author's group developed simplified 3D FEM models using CAD data of knee prosthesis clinically used, and investigated effects of deep knee flexion and internal rotation on the stress state of the tibial inserts [10,11]. In these studies, however, the movement of the tibial inserts of the FEM models was completely restricted and, for example, roll-back behavior in the PS type model was introduced compulsory by moving the femoral component [11].

The aim of the present study is therefore to reproduce more natural roll-back behavior using a simple FEM model of PS type knee prosthesis, and to characterize the stress states of two different types of PS type knee prostheses with different Post and Cam design under deep flexion. 3D FEM models of the knee prostheses were developed from their CAD data. Nonlinear spring model and load data for deep squatting were utilized to simulate more precise knee motion than the motion previously analyzed [11]. Effects of wide range of flexion on the stress state of the condylar surfaces and Post of the tibial inserts were then assessed using the analytical results, and the 1st and the 2nd were compared to characterize the effect of the design modification on reduction of stress concentration and improvement of flexion angle.

2. Development of Finite Element Models

In this study, two different types of PS type knee prosthesis, Stryker Scorpio Superflex and Scorpio NRG, were analyzed to examine the effects of the design difference on the stress distribution in the tibial inserts. Superflex is called the 1st model and NRG the 2nd model, thereafter. The 2nd model, which is clinically used currently, can be recognized as a modified version of the 1st model, and especially, the shape of Post and Cam were redesigned to reduce stress concentration. Post of the 2nd has more round shape than that of the 1st, and the contact surface area of Cam to Post was modified to be larger in the 2nd than in the 1st. 3D-FEA models of the 1st and the 2nd consisting of femoral component, tibial component and tibial insert were constructed from their CAD data obtained from the manufacturer. In this modeling, the tiny parts of the femoral component and the stem of the tibial components were removed prior to finite element meshing in order to avoid extremely small meshes and reduce the number of meshes. It is noted that those removed parts were carefully chosen so that the removal did not affect on the simulation results. The simplified models of the PS type prostheses are shown in Fig.1.

Finite element meshed models are shown in Fig.2. The numbers of the nodes and the elements are 21958 and 89322 for the 1st model and 28254 and 121604 for the 2nd model, respectively. The material constants used in the analysis are shown in Table 1. The tibial insert originally made from UHMWPE (Ultra High Molecular Weight Polyethylene) was assumed to be an elastic-plastic material and to follow the von Mises yield criterion. The nonlinear stress-strain relationship experimentally obtained is shown in Fig.3 [7]. The femoral component made from Co-Cr alloy and the tibial component made from Ti alloy are much stiffer than UHMWPE, and therefore, assumed to be rigid body in order to reduce computational time. The friction coefficient between the femoral component and the tibial insert was chosen to be 0.04 [5]. It was assumed that the back surface of the tibial insert was perfectly connected to the top surface of the tibial component and therefore, the both surfaces possessed the nodes in common.

In a PS type knee prosthesis attached in a real human knee, reaction and frictional force are generated on the condylar and Post surfaces during motions. In this TKA knee, these forces are balanced with the tensions of the soft tissues existing around the knee; as a result,

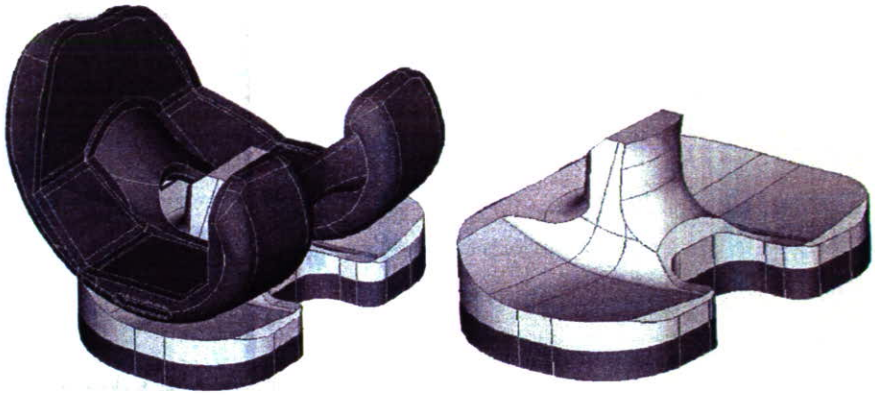

(a) 1st model

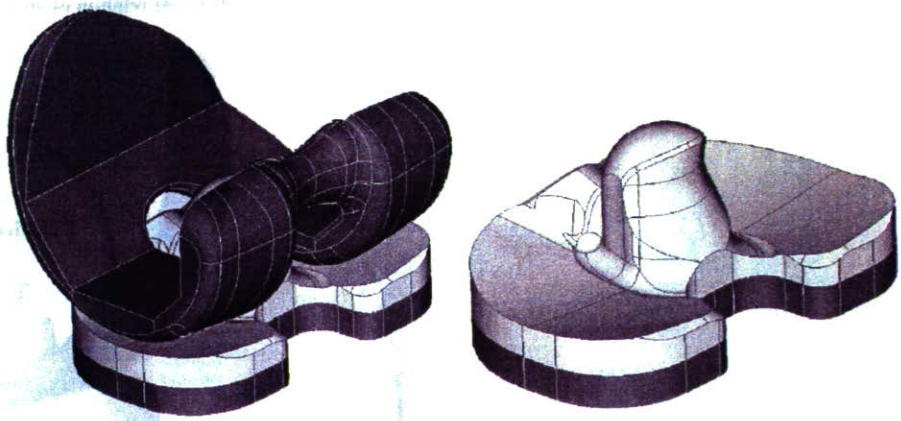

(2) 2nd model

Fig. 1 FEA models of two kinds of PS type knee prostheses.

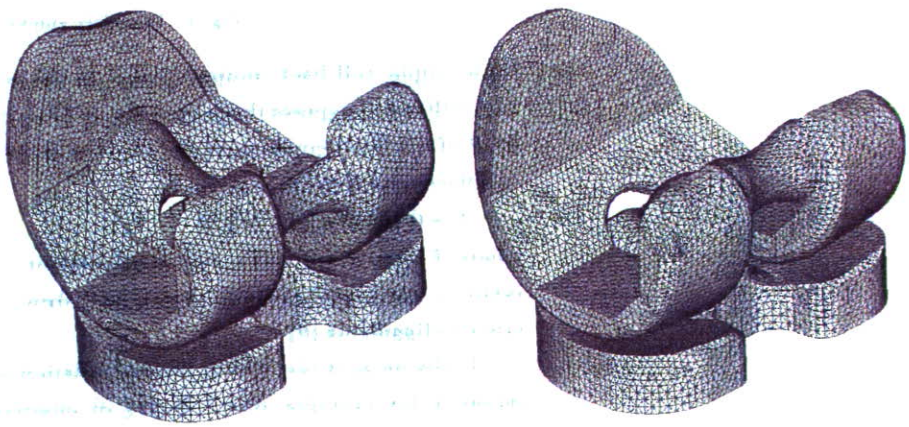

(1) 1st model (2) 2nd model

Fig. 2 FEA mesh models of PS type knee prostheses.

Table 1 Material constants for FEA.

Parts	Material	Density (kg/m^3)	E (MPa)	ν	σ_Y (MPa)
Tibial insert	UHMWPE	940	880	0.4	16

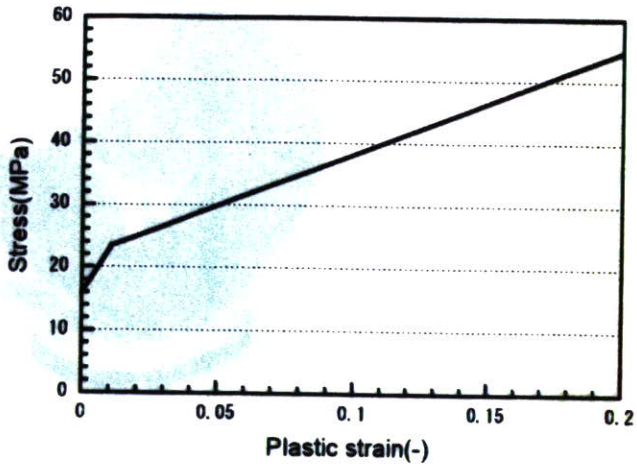

Fig. 3 Bi-linear relation of stress-plastic strain curve of UHMWPE.

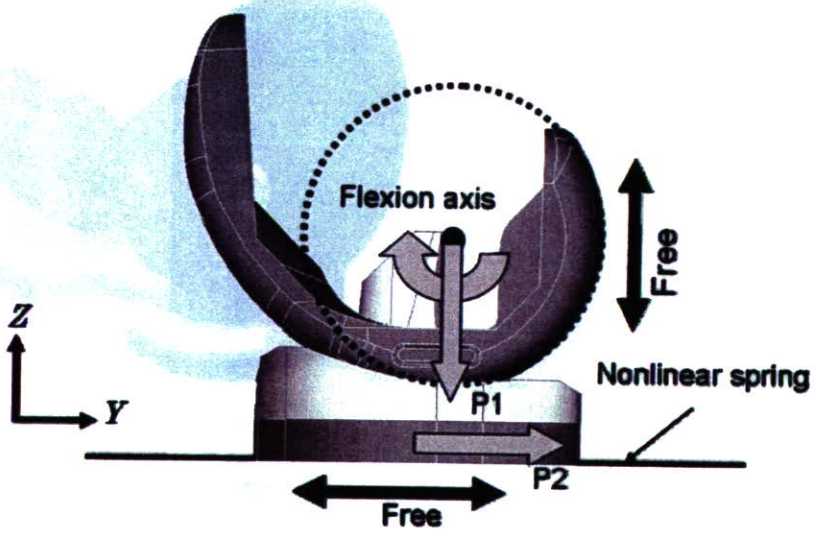

Fig. 4 Boundary conditions of the TKA model.

for example, roll-back motion occurs. In the present FEA models, a nonlinear spring model was utilized to express these motions in TKA [8]. Two spring elements were attached in the front of the tibial component and the two in the back as shown in Fig.4. The nonlinear force -displacement relation is given by

$$F = 0.18667d^2 + 1.3313d \quad (1)$$

where F and d are force and displacement, respectively. It is noted that this nonlinear relation was experimentally determined from a knee with removed anterior and posterior cruciate ligaments [8].

In the most of real knees, internal rotation tends to take place during flexion, and it was reported, for example, that 7 degree of internal rotation occurs at a deep flexion angle of about 135 degree [12]. In the present analysis, however, only flexional motion was considered in order to make the effect of the Post-Cam contact on the stress distribution clearer. The axis of flexion was assumed to be located in the center of the circle which coincides with the shape of the condylar surface of the femoral component (see Fig.4). For the femoral component, only the displacement in Z-direction was free and the displacements in X- and Y-directions were fixed. On the other hand, the tibial component was able to move freely in Y-direction and fixed in X- and Z-directions.

Load data used as the mechanical boundary condition was referred from the reference 2 in which load data for rapid deep squatting was analytically obtained using 2 dimensional model of human knee considering muscular forces. The load P1 and P2 were applied to the

femoral component in the vertical direction (Z-direction) and to the tibial component in the horizontal direction (Y-direction), respectively. The relationship between the load data and the flexion angle were shown with the body force used in the analysis in Fig.5.

A commercially available pre-processor FE-MAP was used to develop those 3D FEM models including solidification from the surface data, meshing and setting up of the boundary conditions. A commercial explicit finite element code LS-DYNA was then utilized as solver, and a post-processor LS-POST was used to analyze the FEM results.

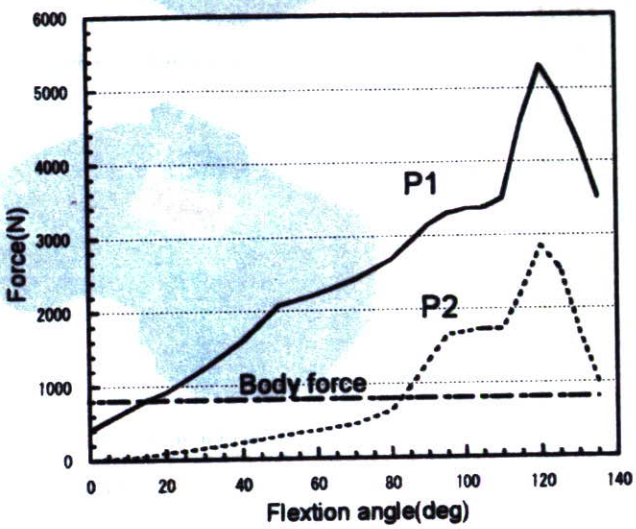

Fig. 5 Force-flexion angle relations used as mechanical boundary condition.

3. Results and Discussion

3.1 Mises equivalent stress distribution

Von Mises equivalent stress distributions of the tibial insert at 45 and 120 degrees of flexion are shown in Fig.6. At 45 degree, stress concentration occurred only on the condylar surfaces, and the maximum stress values of the 1st model and the 2nd model were 11.2 MPa and 17.6 MPa, respectively, indicating that the 2nd exhibited higher maximum stress than the 1st under the same boundary condition. The contact between Post and Cam did not take place at this angle. Larger stress concentration occurred on both the condylar and Post surfaces at 120 degree of flexion. The maximum stress values were 73.0 MPa for the 1st and 48.9 MPa for the 2nd, indicating that stress concentration was effectively reduced in the 2nd at deep flexion angle. It is also noted that the location of stress concentration on the condylar surfaces moved toward the back (Y-direction) as flexion proceeded from 45 to 120 degree, suggesting that roll-back movement was generated. The dependence of the displacement of the spring element on flexion angle is shown in Fig.7. The positive direction coincided with the negative Y-direction in Fig.4. There was no displacement generated up to about 60 degree and the displacement rapidly increased after 60 degree and the final displacement was approximately 12 mm. The difference between the two models was almost negligible. The displacement at the flexion angles greater than 60 degree corresponded to the displacement of the tibial component in the negative Y-direction, that is, so-called roll-back behavior in TKA.

Mises equivalent stress distributions in the cross-sectional areas of the tibial inserts at 120 degree of flexion are shown in Fig.8. It is clearly seen that the stress concentration region with the highest stress level of 40-50MPa was much wider in the 1st model than in the 2nd model. It is also interesting to see that for the 2nd, the highest stress concentration region was located inside of Post, suggesting that the possibility of delamination failure at this point.

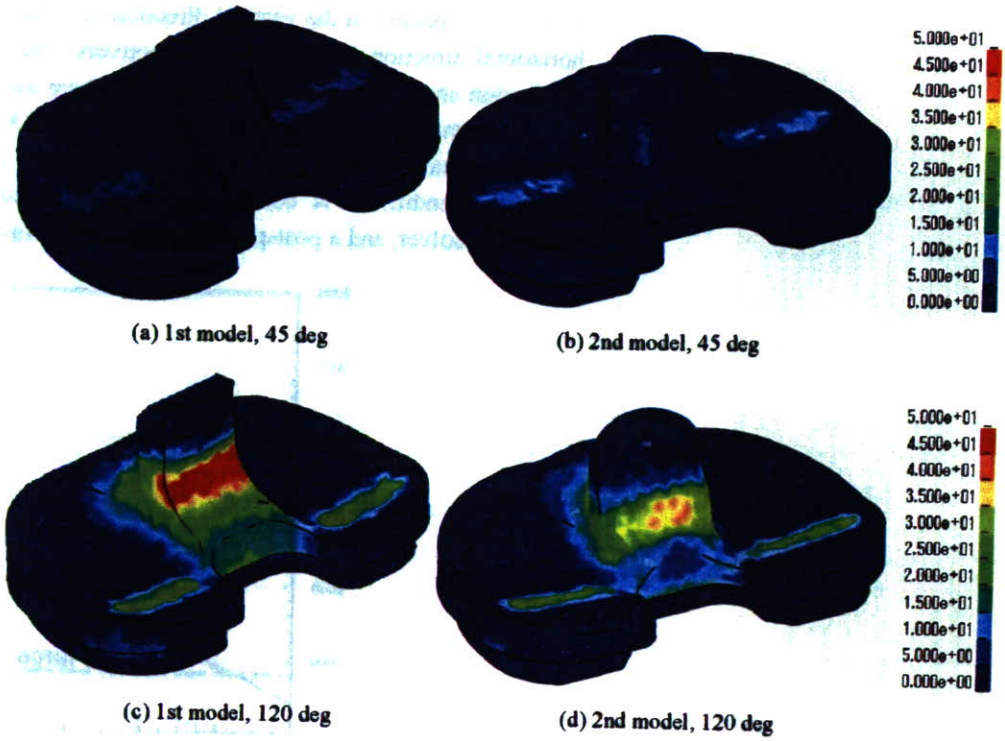

(a) 1st model, 45 deg (b) 2nd model, 45 deg

(c) 1st model, 120 deg (d) 2nd model, 120 deg

Fig. 6 Equivalent stress distribution on the surface of tibial insert (unit: MPa).

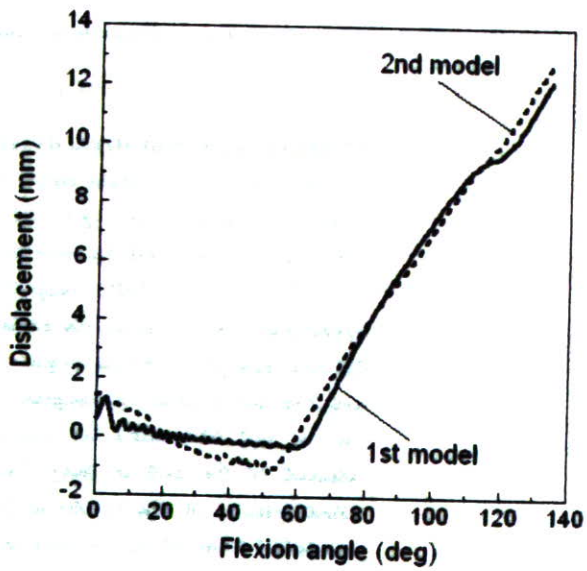

Fig. 7 Dependence of displacement of spring model on flexion angle.

3.2 Dependence of maximum equivalent stress on flexion angle

The dependences of the maximum equivalent stress values on flexion angle on the condylar surface and Post of the tibial inserts are shown in Fig.9. For the condylar surfaces, the maximum stress of the 2nd model was larger than that of the 1st model at flexion angles smaller than 60 degree. On the other hand, the 1st exhibited larger stress at angles greater than 120 degree, however the difference was not so large compared to the Post stress discussed later. The slope of the frontal condylar surface of the 2nd was designed to be a little gentler than that of the 1st; therefore, the contact area between the condylar surfaces of the femoral component and the tibial insert became smaller in the 2nd, resulting in the higher stress at angles smaller than 60 degree. The slope of the rear condylar surface of the 2nd was almost the same as that of the 1st and therefore, the difference of the stress became

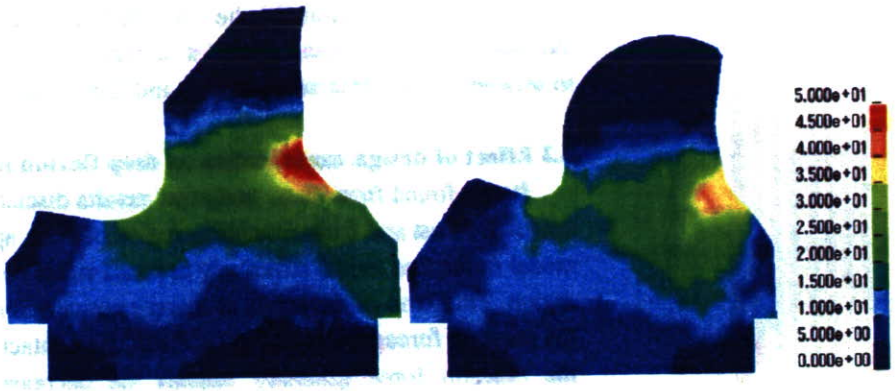

(a) 1st model (b) 2nd model

Fig. 8 Stress distribution in the cross-sectional area of tibial insert at 120 degree of flexion (unit: MPa).

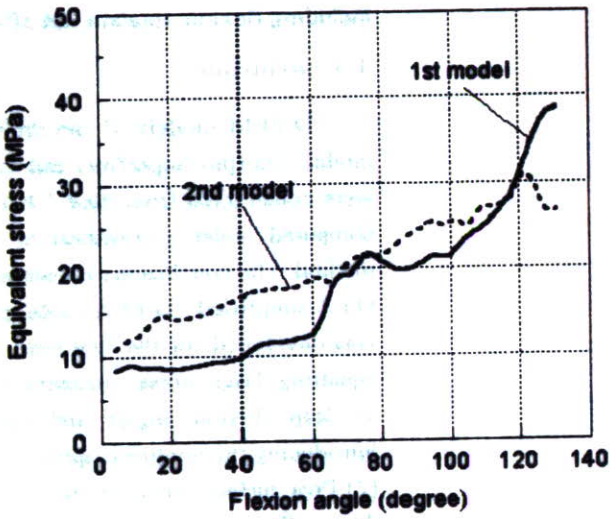

(a) condyle surface

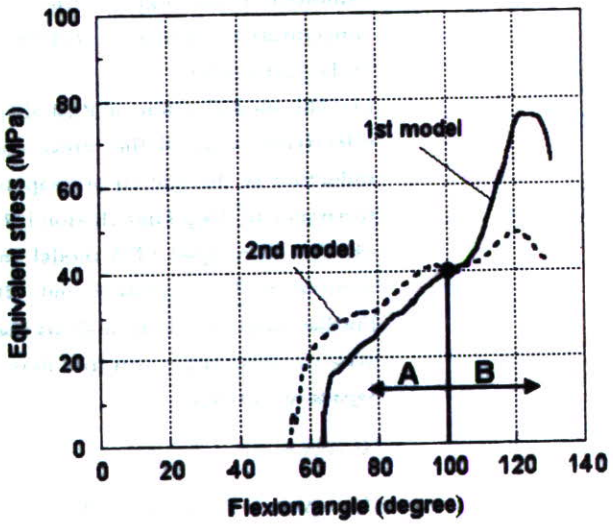

(b) Post surface

Fig. 9 Maximum equivalent stress history on the surface of tibial insert.

small. It was found that the contact between Post and Cam started at 64 degree in the 1st; on the contrary, the contact started at 54 degree in the 2nd. This difference was caused by the difference of the Post shape, i.e., Post of the 2nd was much larger than that of the 1st as a result of the shape modification. The Post surface stress of the 2nd was higher than that of the 1st up to 100 degree (region A in Fig.9(b)); on the contrary, at flexion angles greater

than 100 degree (region B), the 1st exhibited higher Post stress than the 2nd. The rapid increase of the Post stress of the 1st in region B is related to higher stress concentration due to smaller contact area between Post and Cam in the 1st than in the 2nd.

3.3 Effect of design modification on deep flexion motion

It was found from these analytical results discussed above that the design modification, especially Post and the surrounding region of Post, applied in the model change from the 1st model to the 2nd model effectively reduced stress concentration in Post and the surrounding region. This kind of reduction of stress concentration generally corresponds to reduction of the reaction force generated by the Post/Cam contact during deep flexion. Such reduction of the reaction force generally implies the decrease of resistance for deep flexion and therefore, the 2nd model is considered to be more suitable for deep flexion motion than the 1st model. In order to further confirm the superiority of the 2nd model, it is needed to analyze and compare the stress states under more complicated boundary conditions including flexion, rotation and lift-off.

4. Conclusions

3D FEM models of two different types of Stryker's PS type knee prostheses, the 1st model (Scorpio Superflex) and the 2nd model (Scorpio NRG), clinically used worldwide were constructed from their CAD data. Stress states of the two models were analyzed and compared under a condition of deep knee flexion by using the explicit finite element method. The conclusions are summarized as follows:

(1) A simplified 3D-FEA model of PS type knee prosthesis for deep knee flexion analysis was developed for the first time by using nonlinear spring model and load data for deep squatting. High stress concentration due to the Post-Cam contact was reasonably expressed at deep flexion angles and furthermore, roll-back behavior was well simulated by introducing the nonlinear spring model.

(2) Post surface stress of the 2nd model was higher than that of the 1st model up to 100 degree flexion; on the contrary, at flexion angles greater than 100 degree, the 1st model exhibited much higher Post stress than the 2nd model. This is due to higher stress concentration created by smaller contact area between Post and Cam in the 1st model than in the 2nd model.

(3) The modification of Post shape conducted in the designing process of the 2nd model effectively reduced the stress concentration at deep flexion angles. This kind of stress reduction is thought to correspond to the reduction of reaction force, indicating that the resistance to deep knee flexion is lower in the 2nd model than in the 1st model.

(4) The developed FEA model can easily be extended to express more complicated knee motions such as rotation and lift-off through modification of the boundary conditions. Further study on stress analysis under deep knee bending conditions using these models will give us some ideas towards new design concepts for knee prosthesis specially suiting to Japanese lifestyle.

References

(1) Ahir, S.P., Blunn, G.W., Haider H., Walker, P.S., Evaluation of a testing method for the fatigue performance of total knee tibial trays. Journal of Biomechanics, 32(1999), 1049-1057.

(2) Dahlkvis, N.J., Mayo, P., Seedhom, B.B., Forces during squatting and rising from a deep squat, Engineering in Medicine, 11(1982), 69-76.

(3) D'Lima, D.D., Chen, P.C., Kester, M.A., Colwell Jr, C.W., Impact of patellofemoral design on patellofemoral forces and polyethylene stresses, The Journal of Bone and Joint Surgery, 85A(2003), 85-93.

(4) Godest, A.C., Beaugonin, M., Haug, E., Taylor, M., Gregson, P.J., Simulation of a knee joint replacement during a gait cycle using explicit finite element analysis. Journal of Biomechanics, 35(2002), 267-275.

(5) Halloran, J.P., Anthony, J.P., Rullkoetter, P.J., Explicit finite element modeling of total knee replacement mechanics. Journal of Biomechanics, 38(2005), 323-331.

(6) Kanekasu, K., Scorpio Superflex total knee arthroplasty-Design, cilinical results and kinematics, Journal of Joint Surgery, 23(2004), 49-57.

(7) Kobayashi, K., Kakinoki, T., Tanabe, Y., and Sakamoto, M., Mechanical properties of ultra high molecular weight polyethylene under impact comporession - Property change with gamma irradiation and dynamic stress-strain analysis of artificial hip joint - , Journal of The Japanese Society for Experimental Mechanics, 3(2003), 225-229.

(8) Sathasivam, S., Walker, P.S., Computer model to predict subsurface damage in tibial inserts of total knees. Journal of Orthopaedic Research, 16(1998), 564-571.

(9) Morra, E.A., Greenwald, A.S., Polymer insert stress in total knee designs during high-flexion activities: a finite element study. Journal of Bone and Joint Surgery, Am 87(2005), 120-124.

(10) Todo, M., Nagamine, R., Kuwano, R., Hagihara, S., and Arakawa, K., Development of 3D finite element model of total knee arthroplasty and computational efficiency, Japanese Journal of Clinical Biomechanics, 27(2006), 231-237.

(11) Todo, M., Nagamine, R., Yamaguchi, S., Hagihara, S., and Arakawa, K., Effect of flexion and rotation on the stress state of UHMWPE insert in TKA, Japanese Journal of Clinical Biomechanics, 27(2006), 239-246.

(12) Watanabe, T., Yamazaki, T., Sugamoto, K., Tomita, T., Hashimoto, H., Maeda, D., Tamura, S., Ochi, T., and Yoshikawa, H., In vivo kinematics of mobile-bearing knee arthroplasty in deep knee bending motion, Journal of Orthopaedic Research, 22(2004), 1044-1049.

Bull.Natl.Inst.Health Sci.,125, 61-64 (2007)

視力補正を目的としないおしゃれ用カラーコンタクトレンズの細胞毒性

中岡竜介#, 松本富美子*, 宗林さおり*, 柳橋哲夫*, 土屋利江

Cytotoxicity of Various Non-corrective and Decorative Contact Lenses

Ryusuke Nakaoka, Tomiko Matsumoto*, Saori Sourin*, Tetsuo Yanahashi*, and Toshie Tsuchiya

Abstract

Non-corrective and decorative contact lenses can be purchased as sundries without the guidance of medical doctor. Recently, many cases of eye injury by utilizing these lenses have been reported. To estimate their cytotoxic potential to cause eye injury, cytotoxicity tests of the commercially available non-corrective and decorative contact lenses were performed utilizing the V79 cell colony assay. By the colony assays of the lenses and their extracts, it was suggested that two tested lenses out of the ten are cytotoxic. Although preservatives for these lenses in the products showed cytotoxicity, the cytotoxicity of the two lenses is suggested to be ascribed to un-identified materials, which can be extracted to a cell culture medium from them. The results of this study indicate that cytotoxicity of the non-corrective and decorative contact lenses would be better to be evaluated for estimating their biological safety.

Keywords: non-corrective and decorative contact lens, cytotoxicity, extract, preservative

1. 緒言

現在，視力補正を目的としない場合，すなわちファッション目的で目の色を変えるためのおしゃれ用カラーコンタクトレンズには，薬事法が適用されず規制対象外となっているため，インターネットショップや雑貨店を通じた購入が可能となっている．しかしながら，目に装用して使用するという使用方法は，視力補正を目的としたものと同様である．よって，コンタクトレンズの使用未経験者が専門家の適切な指導を受けないまま，また，それら製品の適切な安全性評価・管理がなされないままそれらのレンズを使用するケースが数多く存在する．PIO-NET（全国消費生活情報ネットワーク・システム）には，おしゃれ用カラーコンタクトレンズを用いた結果生じた炎症や角膜障害などの不具合を中心とした申し出情報が寄せられている[1]．また，米国においても同様の障害が報告されている[2]．

#To whom correspondence should be addressed:
Ryusuke Nakaoka; 1-18-1 Kamiyoga, Setagaya-ku, Tokyo 158-8501, Japan; Tel: 03-3700-9264; Fax: 03-3707-6950; Email: nakaoka@nihs.go.jp
* 独立行政法人国民生活センター商品テスト部 Products Testing Department, National Consumer Affairs Center of Japan

視力補正を目的としないものであっても，コンタクトレンズである以上，本来はその適切な装用法や管理手段の指導を受けるべきであり，報告された不具合はその不適切な使用法が一因であることが大いに考えられる．加えて，その製造や販売にあたり使用部位を考えた場合に行うべき安全性評価・管理がなされないまま，流通していることも予想される．すなわち，PIO-NETに報告されている不具合の原因がおしゃれ用カラーコンタクトレンズ自体の生物学的安全性欠如であることも予想される．

そこで，本研究では，現在入手可能で，ある程度その製造者や材料などが特定できるおしゃれ用カラーコンタクトレンズ10種類を対象として，それらが眼組織に障害を与える可能性を検討するために，眼組織刺激性との相関が報告されている細胞毒性[3]を評価する試験を行ったので，それらの結果について報告する．

2. 実験

2. 1 試料

今回対象としたおしゃれ用カラーコンタクトレンズをTable 1に示す．対象としたレンズは，全て国内で購入可能なものであり（個人輸入を含む），青系4銘柄，茶系4銘柄，それらの色以外の2銘柄，合計10銘柄を入手した．

Table 1. A list of non-corrective and decorative contact lenses utilized for this study

Sample No.	Color	Made in	Materials and Water contents	Basecurve (mm)	Diameter (mm)	Su
1	Blue	South Korea	Polymacon : 62% Water : 38%	8.6	14	
2		South Korea	PHEMA Water : Unknown	8.6	14	
3		Un-identified*	Co-polymer : 58% (HEMA & MMA) Water : 42%	8.6	14	
4		Taiwan	PHEMA Water : Unknown	8.6	14	
5	Brown	UK	Methafilcon : 45% Water : 55%	8.7	14.4	
6		Un-identified*	Co-polymer : 58% (HEMA & MMA) Water : 42%	8.6	14	
7		UK	Filcon 1B : 45% Water : 55%	8.8	14.4	
8		Singapore	HEMA Co-polymer : 45% Water : 55%	8.6	14.2	
9	Violet	UK	Filcon 1B : 45% Water : 55%	8.8	14.4	
10	Red	UK	Filcon 1B : 45% Water : 55%	8.8	14.4	

* "Materials from USA" is only described on the package of the product.

HEMA: 2-Hydroxyethyl methacrylate
MAA: Methacrylic acid
PHEMA: Poly HEMA
Polymacon: PHEMA (USAN)
Methafilcon A, Etafilcon A: Copolymer of HEMA and MAA (USA
Filcon 1B: ISO category of hydrogel material made from copolyme
Phemfilcon A: Copolymer of HEMA and EOEMA (USAN)
EOEMA: 2-Ethoxyethyl methacrylate

2. 2 細胞毒性試験

細胞毒性試験は，厚生労働省の生物学的安全性試験ガイドライン[4]，ISO関連文書[5]及び細胞毒性試験に関する報告[3, 6, 7]を参考にして，承認申請時に求められるものに準拠した方法で行った．細胞はChinese hamster lung fibroblasts（V79細胞）を用い，Eagle' s minimal essential mediumに10 %のウシ胎児血清（FCS）を加えたもので，37° C，5 % CO2培養器中で継代したものを実験に使用した．

具体的な細胞毒性試験手法を以下に示す．試験には，Earleの平衡塩類溶液培地に非必須アミノ酸，ピルビン酸ナトリウム（0.11 g/l），L-グルタミン（0.292 g/l），炭酸水素ナトリウム（2.2 g/l），ペニシリン・ストレプトマイシン及びFCS 5 %を含んだ培地（M05培地）を使用した．24-well プレート（Corning Inc., Corning, NY）に静置した孔径0. 4 μmの tissue culture insert（Nunc A/S, Rocklide, Denmark）中にV79細胞を約25個懸濁させた500 μlのM05培地を加え，さらにinsertを入れたwellに500 μlのM05培地を加え4時間培養して細胞をinsertに接着させた．検体となるコンタクトレンズは，予め別の24-wellプレート中に静置して準備しておいた．V79細胞が接着したinsertを内部の培地を除いた後に速やかに検体入りのプレートに移し，well中及びinsert中にそれぞれ500 μl，合計1 mlのM05培地を加えてさらに培養を行った．1週間後，Giemsa染色を行い，染色されたコロニー数を計測した．なお，試験の検出感度と精度を確認する目的で，細胞毒性試験用の陰性対照材料及び陽性対照材料を用いての試験も同時に行った．陰性対照材料としては組織培養用プラスチックシート（和光純薬製）を，陽性対照材料としては0.1 % zinc diethyldithiocarbamate（ZDEC）含有ポリウレタンフィルム（PU）（陽性対照材料A），0.25 % zinc dibutyldithiocarbamate（ZDBC）含有PU（陽性対照材料B）を（財）食品薬品安全センター秦野研究所より入手して用いた．コンタクトレンズの細胞毒性は検体の入ってないinsert中でのコロニー数を100 %として，各insert中に観察されたコロニー数を比較することで評価した．

次に，上記の方法で細胞毒性があることが疑われたレンズを中心にいくつかのおしゃれ用カラーコンタクトレンズを選び，滅菌プラスチックチューブにそれらのレンズ各10枚を入れレンズ表面積に対して6 cm^2/mlになる量のM05培地を加えた．それらのチューブを24時間細胞培養器中に静置することでレンズ抽出液を調製した．24-well プレートにV79細胞を50個/well/500 μl M05培地で播種して4時間培養を行った後に培地を捨て，調製したレンズ抽出液をM05培地で段階希釈したものを500 μl加えてさらに培養した．1週間培養後に形成されたコロニー数を計測し，抽出液未添加の場合に計測されたコロニー数と比較することで調製したレンズ抽出液の細胞毒性を評価した．

また，各製品のパッケージ中にレンズ保存用としてレンズと共に入っていた保存液の毒性は以下の方法で評価した．24-wellプレートにV79細胞を50個/well/500 μl M05培地で添加して4時間培養後培地を捨て，回収した保存液を添加して段階希釈したM05培地を加えて1週間培養後の形成コロニー数からその毒性を評価した．抽出液及び保存液の試験では，前記2種類の陽性対照材料A及びB，陰性対照材料に加えて陽性対照物質であるZDBCとを試験系の感度及び精度確認のために使用した．

なお，得られたデータはDunnettの多重比較による検定を行い，検体を加えていないコントロール群との有為差を必要に応じて示した．

3. 結果及び考察

コンタクトレンズの使用法を考慮した場合，細胞と直接接触させてその細胞毒性を検討する直接接触法を行うことが理想ではあるが，今回の対象レンズが全てソフトコンタクトレンズのため細胞接着性が低いこと，またレンズ自体は平面でなく眼球に合わせた曲率を持ち材料への均一な細胞播種が不可能であるため，実際のコンタクトレンズ承認申請時にも使用されているtissue culture insertを利用した試験を行った．

Table 2に，コロニー法を用いて算出した細胞毒性試験の結果を示す．

Table 2. Cytotoxicity of various non-corrective and decorative contact lenses estimated by V79 cell colony assay utilizing a tissue culture insert (All data are expressed as an average percent ratio against that of a control group ± S.D. (n=3))

Sample No.	Viability of V79 cells (% vs control)
1	119.6 ± 12.9
2	117.5 ± 12.4
3	96.9 ± 9.4
4	101.0 ± 21.7
5	105.2 ± 16.4
6	*33.0 ± 19.9* *
7	113.4 ± 28.6
8	101.0 ± 12.9
9	113.4 ± 9.4
10	94.8 ± 21.7
Negative Reference Material	
Polystyrene	84.5 ± 7.1
Positive Reference Materials	
ZDEC	0.0 ± 0.0 *
ZDBC	0.0 ± 0.0 *
Control	100.0 ± 18.1

Italic number: Observed colonies are very small compared to that observed in a control group
* p< 0.01 against a control group

コロニー形成率の明らかな低下が認められたものはNo.6のみで，その他のコンタクトレンズではコロニー形成率の低下は認められなかった．

No.6のレンズによるコロニー形成率低下の原因に関してさらに検討を加える目的で，No.6を含めていくつかのレンズを選び，それらのレンズから調製した培地抽出液の毒性を検討した（Fig.1）．なお，別に細胞代謝活性評価を行ってその低下が認められなかったレンズ（No.1, 2及び7）は細胞への悪影響がないと判断し（未公開データ），この検討からは除いている．Fig.1から明らかなように，No.3及び6の抽出液においてコロニー形成率の低下が認められ，算出したそれぞれのIC50は約80 %，89 %であった．

Table 2に示されるinsertを用いた試験ではNo.3の細胞毒性が検出されなかったが，これはこの試験での抽出条件が3.5から4.2 cm^2/mlの表面積/抽出培地比であり，レンズ抽出液調製時と比較して表面積/抽出培地比が小さい抽出条件下であったことが一因と考えられる．Fig.1において，この比に相当する抽出液濃度（58 %）でのコロニー形成率はNo.3では同レベルであったが，No.6では高くなっている．このことから，No.6では時間とともにより多くの細胞毒性物質が培地中に溶出されており，その結果，Table 2で示されたように毒性が検出されたと考えられる．よって，表面積/培地比を同じにすることが可能であれば，insertを用いた試験法は抽出液を用いた手法よりも感度が高い手法であると考えられるが，insertを用いた試験法で評価する場合，IC50で細胞毒性強度を定量的に示しうる抽出液を用いた試験法との併用が望ましいことも示された．

抽出液でコロニー形成率の低下が認められたNo.3及び6と形成率低下が認められなかったもののうち No.5及び10の保存液の細胞毒性を検討した（Fig.2）．その結果，No.3及び6の保存液でコロニー形成率の減少が認められ，これらの保存液に細胞毒性があることが示された．製品パッケージや説明書にはこの保存液の詳細に関する記述はないが，長期保存を可能にするための防腐剤などが含まれている可能性があり，レンズ中に残存している保存

Fig. 1. Cytotoxicity of extracts prepared from various non-corrective and decorative contact lenses. All data are expressed as average percent ratio against that of a control group (without adding the extracts) ± S.D. (n= 4).
* p< 0.01 against the result obtained from a control group

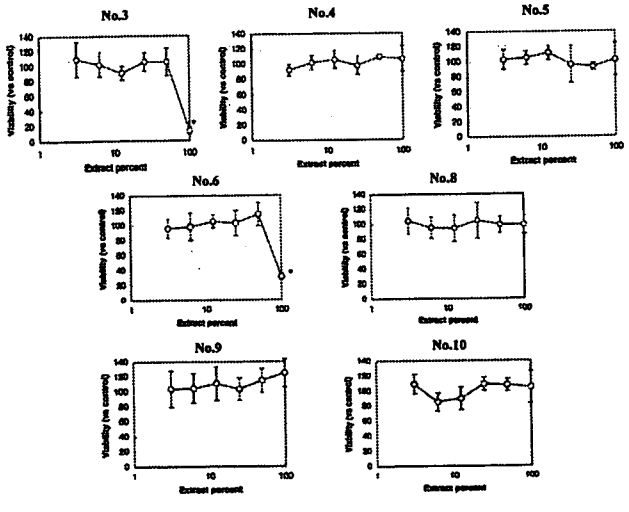

Fig. 2. Cytotoxicity of preservatives for various non-corrective and decorative contact lenses. All data are expressed as average percent ratio against that of a control group (without adding preservatives) ± S.D. (n= 3). Upper figures are results of preservatives of the lenses from which extracts did not show cytotoxicity. Lower figures are results of preservatives of the lenses from which extracts showed cytotoxicity
* p< 0.05, ** p< 0.01 against the result obtained from a control group

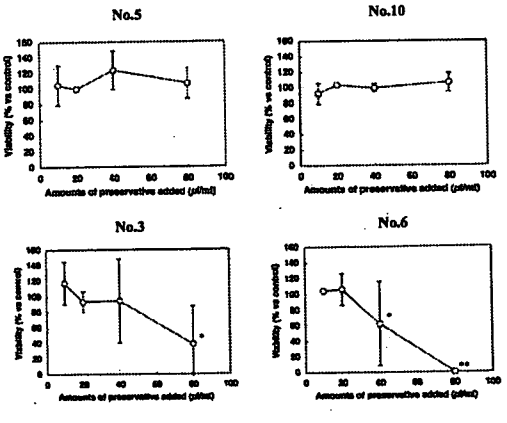

液中の防腐剤に起因した細胞毒性のためにコロニー形成率が低下している可能性は否定できない．このレンズの正確な含水量は不明であるが，今回用いたレンズで含水率が明記されていたもので最も高い含水率 55 %のレンズの場合には，そのレンズ中の保存液量は多く見積もっても19.9 μl程度となることが分かっている．抽出液は10枚のレンズに対して6.9 mlの培地を加えて調製していることから，含水率55 %の100 %レンズ抽出液中の保存液の濃度は約28.0 μl/mlと算出できる．No.3及び 6のレンズ含水率は42 %であるため，上述したレンズ抽出液と比べ，保存液濃度は低いと考えて差し支えない．よって，含水率55 %での最大濃度である28.0 μl/mlを超えることは考えられず，No.3 及び6の保存液濃度がその濃度(28.0 μl/ml) であっても100 %抽出液で見られたようなコロニー形成率の大きな低下は認められないことから，No.3及び6の抽出液で示されたコロニー形成率の低下は，保存液中にもともと含まれている可能性のある防腐剤などではなく，レンズ材料から抽出される物質，すなわちコンタクトレンズ自体に起因したものであることが予想される．

では，このコロニー形成率の低下を示した物質は何であろうか？保存液中の溶出物に関して検討した結果，ほぼ全てのレンズの保存液中にメタクリル酸モノマーが検出されること，しかしながら，メタノールを用いた溶出試験からメタクリル酸モノマーのさらなる溶出はなかったこと，一方，細胞毒性が示唆されたNo.3及び6と細胞毒性が認められなかったNo.9及び10ではいずれも色素が溶出することが報告されている[1]．Fig.2の結果と報告されているモノマー量[1]との間には相関が見られなかったことから，メタクリル酸モノマーが細胞毒性の原因である可能性は小さい．しかしながら，メタクリル酸やメタクリル酸2-ヒドロキシエチルモノマー，あるいはこれらのモノマーからなる低分子量のオリゴマーが培地中に溶出している可能性は否定できない．また，溶出が認められた色素の毒性に関しては全く未知であるが，No.3及び6に使用されている色素が細胞毒性試験中に培地中に溶出してくることによりこれらのレンズが細胞毒性を示している可能性もある．特に，血清含有培地での抽出では，水溶液での抽出に比べてより脂溶性の高い物質が溶出されることもあり，No.3及び6には細胞毒性のある何らかの物質が材料中に残存している可能性が考えられ，さらに詳細な分析を行う必要がある．

以上，本研究に用いた検体中でコンタクトレンズ自体に細胞毒性があると考えられるものはNo.3と6であった．おしゃれ用カラーコンタクトレンズの使用に伴う不具合の症状は詳細に報告されているものの，今回用いたレンズが実際に不具合を起こしたものと同じであるかは不明である．

また，一部のコンタクトレンズ製品中の保存液には細胞毒性が認められた．今回認められたコンタクトレンズの細胞毒性との関連性はほとんどないと判断されたものの，その組成に関する詳細な記載がないことから，保存液で観察された毒性の原因について判断及び考察を行うことができなかった．防腐剤などが添加されていることは，有効期限が数年になるものもあることから容易に想像はできるものの，その化学物質が目への適用が認められているかどうかなどが明らかにされていないことは，規制対象外の製品とはいえ問題である．毒性物質のレンズへの吸着による眼粘膜への毒性作用の持続なども危惧されるため，レンズの保存液に関しても，今後は詳細な記載を要望するなど何らかの対応が必要かもしれない．

おしゃれ用カラーコンタクトレンズによる不具合は，これらの細胞毒性だけでなく材質の様々な特性にも起因する可能性が，本研究で細胞毒性が示されなかったレンズを用いての装用試験によって示唆されている[1]．角膜層はデリケートな部位のためレンズの物性や形状によっては簡単に障害を生じることを考慮すると，おしゃれ用カラーコンタクトレンズの使用には様々なリスクが潜在していると思われるため，今回行ったような細胞毒性試験を含む生物学的安全性評価を行うことが望ましいのではないだろうか．

参 考 文 献

1) 独立行政法人国民生活センター報道発表資料「おしゃれ用カラーコンタクトレンズの安全性 −視力補正を目的としないものを対象に−」 平成18年2月
2) FDA News for immediate release P02-43, October 21, 2002
3) Tsuchiya, T., Arai, T., Ohhashi, J., Imai, K., Kojima, H., Miyamoto, S., Hata, H., Ikarashi, Y., Toyoda, K., Takahashi, M. and Nakamura, A.: J. Biomed Mater Res., 27, 885-893 (1993)
4) Guidelines for preclinical biological evaluation of medical materials and devices. Ministry of Health, Labour and Welfare memorandum, JIMURENRAKU Iryokiki-Shinsa No. 36 (2003.3.19).
5) ISO10933-5: 1999, Biological evaluation of medical devices - Part 5: Tests for in vitro cytotoxicity
6) Tsuchiya, T., Ikarashi, T., Arai, T., Ohhashi, J. and Nakamura, A.: J Appl Biomater., 5, 361-367 (1994)
7) Tsuchiya, T., Ikarashi, Y., Arai, T., Ohhashi, J., Isama, K. and Nakamura, A.: Clinical Mater., 16, 1-8 (1994)

Rheumatology 2007;46:1652–1656
Advance Access publication 12 September 2007

doi:10.1093/rheumatology/kem220

Serum keratan sulfate is a promising marker of early articular cartilage breakdown

S. Wakitani[1], M. Nawata[2], A. Kawaguchi[1], T. Okabe[3], K. Takaoka[1], T. Tsuchiya[4], R. Nakaoka[4], H. Masuda[5] and K. Miyazaki[5]

Objectives. To find serum markers that may serve as indices for an early diagnosis of degeneration or damage of the articular cartilage.
Methods. Twenty-four healthy volunteers, 19 individuals with knee trauma (KT) and 31 with knee osteoarthritis (OA) were evaluated. KT patients were divided into a group ($n=5$) with an injury <2 months old (recent KT) and a group ($n=14$) with that >2 months old (old KT). Articular cartilage damage was assessed using either arthroscopy or direct observation. Serum concentrations of hyaluronic acid (HA), cartilage proteoglycan aggrecan turnover epitope (CS846) and cartilage oligomeric protein (COMP) were measured using enzyme-linked immunosorbent assay kits and those of keratan sulfate (KS) and chondroitin-6-sulfate (C6S) using high-performance liquid chromatography.
Results. Serum KS in the recent KT group (2095 ± 594 ng/ml) was significantly higher than that in the old KT group (1373 ± 418 ng/ml; $P=0.021$), and serum COMP in the recent KT group (1572 ± 182 ng/ml) showed a tendency that was higher than that in the old KT group (1350 ± 250 ng/ml; $P=0.079$).
Serum KS in OA patients with Kellgren and Lawrence (KL) grades 0 and I (1456 ± 334 ng/ml) showed a tendency that was higher than that in OA patients with KL grades II, III and IV (1248 ± 220 ng/ml; $P=0.084$).
Conclusions. The serum concentration of KS correlated with the damage of the articular cartilage and it was significantly increased even at an early stage after the injury.

KEY WORDS: Keratan sulfate, Glycosaminoglycan, Cartilage oligomeric protein, Cartilage injury, Osteoarthritis, Serum marker.

Introduction

The prevalence of patients with articular cartilage defects among patients with symptomatic knees requiring arthroscopy has been reported as 5–20% [1–3]; when left untreated, osteoarthritic changes are observed on X-rays taken after 10–20 yrs [4, 5]. Thus, articular cartilage injury is considered a cause of osteoarthritis (OA). Even if there is no articular cartilage injury, degeneration of the articular cartilage is considered to begin in humans at a young age, and articular cartilage changes, such as changes in colour and fibrillation, can occur. Injury or early-stage alterations of the articular cartilage in OA cannot be detected using X-ray examination. Magnetic resonance imaging (MRI) can detect articular cartilage defects and cartilaginous quality changes to some extent, but this technique is not sensitive enough to detect early OA changes and is expensive to be used as a routine examination. Serum markers, on the other hand, are suitable as screening tests, and only patients with high values of serum markers should be subjected to MRI or arthroscopy to detect articular cartilage degeneration. If it were possible to detect OA or articular cartilage damage at an early stage, patients could be educated to prevent the progression of OA. Moreover, it would be useful to monitor the natural course of articular cartilage damage or repair after, for instance, autologous chondrocytes implantation, whose effectiveness is still controversial because there is no method to effectively evaluate cartilage repair.

In 1985, Thonar *et al.* [6] measured serum keratan sulfate (KS) using an enzyme-linked immunosorbent assay (ELISA) by anti-KS antibody (1/20/5-D-4), and suggested its usefulness as a marker of OA. However, the correlation was weak and it did not correlate with X-ray grading [7]. Many researchers have tried to detect the metabolic products of articular cartilage components (proteoglycan, type II collagen and non-collagenous proteins) in joint fluid or blood and thereby a marker of OA [8–11]. As reported by Okumura *et al.* [12], early OA articular cartilage destruction begins with a loss of glycosaminoglycans (GAGs) from articular cartilage surfaces, followed by collagenolysis. Thus, the first event in OA or articular cartilage damage is the release of GAGs, which play an important role in maintaining articular cartilage function. Consequently, early markers of articular cartilage damage or OA change might be among GAG metabolic products. We selected KS, chondroitin 6 sulfate (C6S), cartilage proteoglycan aggrecan turnover epitope (CS846) and hyaluronan (HA) as candidate markers, and cartilage oligomeric protein (COMP), which is not a component of GAGs but has been reported to be a marker of OA [9]. These components have been reported to correlate with OA, to some extent, but not with cartilage damage caused by degradation and/or injury. These metabolic products can be measured in joint fluid, serum and urine, but we measured them in serum because it is easy to collect.

We measured KS using high-performance liquid chromatography (HPLC), which has been reported to be more accurate than ELISA [13]; C6S using HPLC, and CS846, HA and COMP using ELISA. We measured these markers in healthy volunteers and in patients with knee trauma (KT) or OA, who were subjected to knee surgery and whose articular cartilage was optically assessed (by arthroscopy or direct observation). We examined the correlation of these markers with the articular cartilage assessment to evaluate their usefulness as markers of early articular cartilage breakdown caused by degeneration and/or injury but that showed no change by X-ray examination.

Patients and methods

This study was approved by the institutional Review Board of Marunouchi Hospital and was conducted in accordance with the Helsinki Declaration of 1975, revised in 1983. Written informed consent was obtained from the healthy volunteers and patients prior to their participation in the study.

[1]Department of Orthopaedic Surgery, Osaka City University Graduate School of Medicine, [2]Department of Orthopaedic Surgery, Marunouchi Hospital, [3]Department of Orthopaedic Surgery, Shinshu University School of Medicine, [4]Division of Medical Devices, National Institute of Health Sciences and [5]Department of Pharmaceuticals information, Seikagaku Corporation.

Submitted 11 April 2007; revised version accepted 19 July 2007.

Correspondence to: Shigeyuki Wakitani, MD, Department of Orthopaedic Surgery, Osaka City University Graduate School of Medicine, 1-4-3 Asahi, Abeno-ku, Osaka 545-8585, Japan. E-mail: wakitani@med.osaka-cu.ac.jp

Blood collection from healthy volunteers

Ten men and 14 women (23–52 yrs old) volunteered to participate in the study. The volunteers were healthy with no gross obesity, inferior limb malalignment, history of knee injury or knee disorders. Sera were collected and stored at −80°C.

Patients with KT or knee OA

Nineteen KT patients (11 men and 8 women; 20–54 yrs old) and 31 patients with knee OA (11 men and 20 women; 40–80 yrs old) who were diagnosed to undergo knee surgery participated in the study. X-rays of knee and lumbar spine were available for all the patients. Sera samples were collected before surgery and stored at −80°C. The condition of the knee articular cartilage was observed at the time of surgery either arthroscopically or by direct observation. Among the 19 KT patients, two had meniscal injuries, 12 had ligament injuries and five had both meniscal and ligament injuries. KT patients were divided into a group of 5 patients with injuries <2 months old (recent KT) and a group of 14 patients with injuries >2 months old (old KT). Among the 31 OA patients, eight underwent total knee replacement, one underwent a high tibial osteotomy and 22 underwent arthroscopic debridement.

Assessment of articular cartilage surfaces by X-ray and visual inspection

X-ray images were assessed using the Kellgren and Lawrence (KL) grading scale [14]. All the KT patients were KL grade 0. Seven of the OA patients were KL grade 0, seven were KL grade I, four were KL grade II, six were KL grade III and seven were KL grade IV. Articular cartilage damage was assessed using the Societé Francaise d' Arthroscopie (SFA) scaling system [15]. In brief, the degree of articular cartilage damage was estimated from 0 to IV according to the SFA grading scale. The width of the damaged area was evaluated as a percentage of the damaged area in the medial and medial femoro-tibial and patello-femoral areas, separately. The SFA score was then calculated using a coefficient. The SFA score represents not only the degree of articular cartilage surface damage, but also the width of the damaged area.

Determination of the serum markers

Keratan sulfate was determined by HPLC after digestion with keratanase II (Seikagaku Corporation, Tokyo, Japan) according to the method of Tomatsu *et al.* [13] Each serum sample (0.2 ml) was treated with a protease (actinase E: Kaken Pharmaceutical Co. Ltd., Tokyo) and the negatively charged substance containing KS was fractionated by Q sepharose and digested by keratanase II. The KS-derived β-galactosyl-(1-4)-6-*O*-sulfo-*N*-acetylglucosamine (m-ks) and β-6-*O*-sulfo-galactosyl-(1-4)-6-*O*-sulfo-*N*-acetylglucosamine (d-ks) were contained in the solution that was digested by the enzyme and were measured using HPLC. Standard KS derived from bovine cornea (Seikagaku) was used to measure KS under identical conditions; and the quantity of KS in each serum sample was calculated as the sum of m-ks and d-ks. To determine C6S concentration, 0.2 ml of each serum sample was first treated with chondroitinase ABC (Seikagaku). The quantity of unsaturated disaccharide contained in the digested fluid was determined and C6S was detected by HPLC [16]. For the determination of CS846, COMP and HA, the Aggrecan Chondroitin Sulfate 846 Epitope ELISA Kit (IBEX Technologies, Inc., Montreal, Quebec, Canada), Human COMP ELISA Kit (Kamiya Biomedical Company, Seattle, WA, USA) and Hyaluronan Assay Kit (Seikagaku Corporation) were used respectively.

Statistical analysis

To determine the statistical significance of inter-group differences, Steel's multiple comparison test for patient group *vs* control and Wilcoxon rank-sum test for inter-patient group were conducted, and the *P*-level was set at <0.05.

Results

Arthroscopic findings in KT patients and serum concentrations of KS, C6S, CS846, HA and COMP

All KT patients had articular cartilage damage. Their cartilaginous damage scores (SFA) for the recent KT group and the old KT group were 1.2 ± 0.7 and 3.8 ± 3.9, respectively. On X-ray examination, no changes were noted in the knee or intervertebral joints (Fig. 1).

The serum concentrations of KS, C6S, CS846, HA and COMP in KT patients are shown in Table 1. KS, C6S, CS846 and COMP were significantly higher in the recent KT group ($P = 0.001$, $P = 0.047$, $P = 0.022$ and $P = 0.001$, respectively), and KS and COMP higher in the old KT group (both $P < 0.001$) than in controls.

X-ray and arthroscopic examination of OA patients and serum concentrations of KS, C6S, CS846, HA and COMP

The SFA scores of OA patients distributed by their KL grade are presented in Table 2. The SFA score increased in relation with

FIG. 1. Representative radiographs of the knee and lumbar spine and photograph of the articular cartilage in the knee of a 36-yr-old man with traumatic arthropathy. The X-ray grade, SFA score and serum KS concentration were normal, 0.7 and 2537 ng/ml, respectively. The serum KS concentration was high, although damage of the cartilage was minimal.

increased KL grade. Even in patients with KL grade 0 OA, degeneration or damage of the articular cartilage surface was observed by direct optical methods. In such patients, no X-ray findings were detected in the knee nor in the intervertebral discs (Fig. 2).

Serum concentrations of KS were significantly higher in most OA stages (KL grade 0: $P=0.004$, I: $P<0.001$, III: $P=0.004$ and IV: $P=0.008$) and serum COMP were significantly higher in all OA stages (KL grade 0: $P=0.004$, I: $P=0.002$, II: $P=0.008$, III: $P=0.002$ and IV: $P<0.001$) than in controls. C6S and HA in patients with KL grade IV were significantly higher than in controls (both $P<0.001$).

TABLE 1. Serum concentration of markers of cartilage degeneration or damage in patients with knee trauma

	Healthy subjects	KT patients	
		Recent trauma[a]	Old trauma[b]
n	24	5	14
SFA		1.2 ± 0.7	3.8 ± 3.9
KS (ng/ml)	910 ± 145	2095 ± 594*	1373 ± 418*
C6S (ng/ml)	97 ± 28	122 ± 10*	104 ± 22
CS846 (ng/ml)	137 ± 24	214 ± 77*	142 ± 46
COMP (ng/ml)	1030 ± 150	1572 ± 182*	1350 ± 250*
HA (ng/ml)	41 ± 15	44 ± 19	39 ± 12

The values are the mean ± S.D.
[a]Patients evaluated within 2 months after the injury.
[b]Patients evaluated >2 months after the injury.
*$P<0.05$ *vs* Healthy subjects (Steel's multiple comparison test).
SFA, Societé Francaise d' Arthroscopie score; KS, keratan sulfate; C6S, Chondroitin-6-sulfate; CS846, cartilage proteoglycan aggrecan turnover epitope; COMP, cartilage oligomeric protein and HA, hyaluronic acid.

Comparison of the serum markers between patient groups

Since the serum concentrations of KS and COMP were higher in most stages of KT and OA than in controls, those differences between stages were compared in Fig. 3. The serum KS in the recent KT group (2095 ± 594 ng/ml) was significantly higher than that in the old KT group (1373 ± 418 ng/ml; $P=0.021$) and those in OA patients with KL grades 0 and I (1456 ± 334 ng/ml) showed a tendency that was higher than that in patients with KL grades II, III and IV (1248 ± 220 ng/ml; $P=0.084$). The serum concentrations of COMP in the recent KT group (1572 ± 182 ng/ml) showed a tendency that was higher than that in the old KT group (1350 ± 250 ng/ml; $P=0.079$), but those in OA patients showed no difference between the patient group with KL grades 0 and I (1639 ± 434 ng/ml) and the patient group with KL grades II, III and IV (1731 ± 355 ng/ml).

Discussion

This study showed that the serum concentration of KS was high in patients with early-stage damage of the articular cartilage undetectable by X-ray imaging. Serum KS may be suitable as a screening test for articular cartilage damage and to monitor the natural course of articular damage or repair.

In the KT patients with recent injuries, KS was significantly higher than in those with old injuries, suggesting that serum

TABLE 2. Serum concentration of markers of cartilage degeneration or damage in OA patients

X-ray grade	Healthy subjects	OA patients				
		0	I	II	III	IV
n	24	7	7	4	6	7
SFA		2.4 ± 2.1	5.1 ± 3.5	28.8 ± 47.5	>100	>200
KS (ng/ml)	910 ± 145	1501 ± 360*	1411 ± 326*	1253 ± 241	1352 ± 242*	1155 ± 176*
C6S (ng/ml)	97 ± 28	116 ± 18	115 ± 15	102 ± 22	131 ± 22	157 ± 53*
CS846 (ng/ml)	137 ± 24	147 ± 67	151 ± 108	140 ± 70	112 ± 16	211 ± 184
COMP (ng/ml)	1030 ± 150	1710 ± 550*	1570 ± 310*	1580 ± 200*	1630 ± 470*	1907 ± 268*
HA (ng/ml)	41 ± 15	80 ± 65	72 ± 21*	76 ± 68	116 ± 76	258 ± 230*

The patients were grouped by their X-ray grade.
The values are the mean ± S.D.
*$P<0.05$ *vs* Healthy subjects (Steel's multiple comparison test).
SFA, Societé Francaise d' Arthroscopie score; KS, keratan sulfate; C6S, chondroitin-6-sulfate; CS846, cartilage proteoglycan aggrecan turnover epitope; COMP, cartilage oligomeric protein and HA, hyaluronic acid.

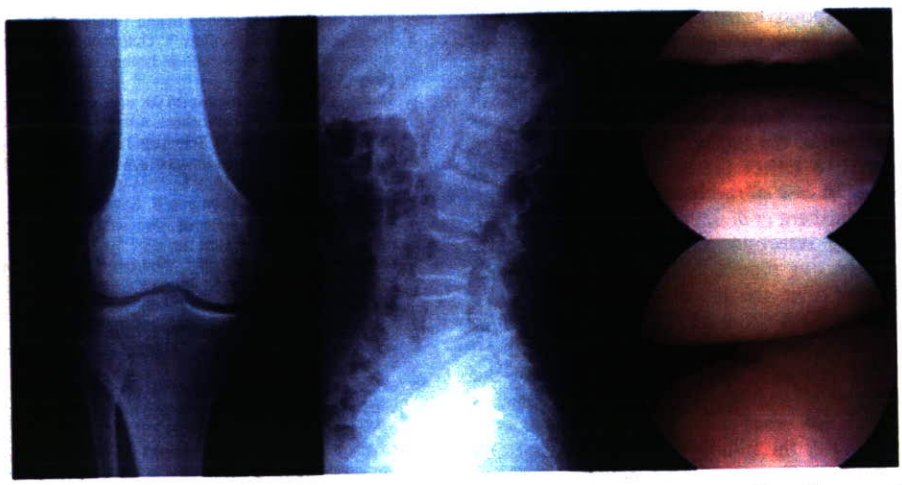

FIG. 2. Representative radiographs of the knee and lumbar spine and photograph of the articular cartilage in the knee of a 66-yr-old woman with KL grade 0 OA. The SFA score and serum KS concentration were 1.7 and 2145 ng/ml, respectively. The serum KS concentration was high, although the patient had early-stage OA.

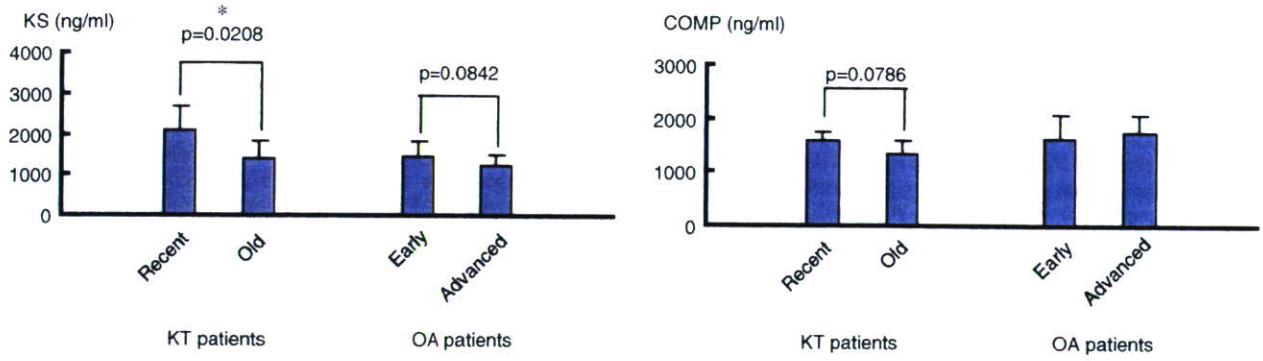

FIG. 3. Comparison of the serum markers between stage groups in KT or OA patients. KT patients were divided into a group with an injury <2 months old (recent) and a group with an injury >2 months old (old). OA patients were divided into a group with KL grades 0 and I (early) and a group with KL grades II, III and IV (advanced). Data are the mean ± S.D. *$P < 0.05$ (Wilcoxon rank-sum test).

KS might indicate the release of cartilaginous GAG in the early stage after injury in spite of moderate cartilaginous damage.

In OA patients, the serum concentrations of KS, C6S, HA and COMP were significantly higher than in healthy controls as reported previously [6, 17–19]. Among these parameters, KS was high in patients with KL grades 0 and I, indicating that KS might serve as a marker of early-stage OA. The KS concentrations in OA patients tended to decrease as the KL grade increased from 0 to IV, which reflects disappearance of the joint space. It may mean that in OA, a greater quantity of the cartilage matrix is released when the joint space has not yet narrowed. On the contrary, COMP was high in KL grade IV. This can be explained by the fact that COMP is a non-collagen protein that exists in the synovial membrane, meniscus and tendon, as well as in the cartilage and its increase is most likely related to the inflammation of various intra-articular tissues. The changes in C6S and HA were marked in KL grade IV, indicating that these are not markers of early-stage cartilage destruction.

KS is a component of proteoglycans found in the articular cartilage, intervertebral discs and corneas. Because corneas are relatively small tissues, serum KS mainly originates from articular cartilage and intervertebral discs. Thus, the serum concentration of KS is not only a marker of knee articular cartilage, but also of other joints and intervertebral discs. Therefore, before concluding that the elevated serum concentration of KS originated from damage to the knee joint articular cartilage, the possibility of spondyloarthropathy and OA in other joints must be examined. We verified that there were no X-ray changes in the lumbar spine nor symptoms caused by lumbar spinal abnormalities in KT patients (Fig. 1), although spondyloarthrotic changes existed in OA patients because most of these patients were of advanced age (Fig. 2). We verified that no OA symptoms were observed in joints other than the knee in these patients. We are planning to investigate serum KS in patients with spondyloarthropathy or intervertebral disk herniation in the future.

Serum KS is considered to reflect the normal metabolism of cartilage, and KS increases in case of mechanical injuries within a few months after injury. Budsberg *et al.* [20] found that serum KS increased 1–3 months after resection of the anterior cruciate ligaments of dog knees. In our report, KT patients who were evaluated within 2 months after the injury exhibited an acute release of KS. Although the SFA score of KT patients was very small, indicating that damage was confined, serum KS was high (Table 1). After the rapid release of KS ends, release from the injured surfaces continues at a relatively high rate. This phase is considered to continue for a few years to a couple of decades as in KT evaluated >2 months after the injury and in early-stage OA patients (KL grades 0 and I). The persistence of this condition leads to OA in a few decades. This phase corresponds to advanced OA (KL grades II, III, IV).

This report is the first study to show that serum KS increases early after an injury causing small articular damage and in patients with early-stage OA undetectable by X-ray imaging. As only a small volume of blood is required for the measurement of serum KS, this parameter may serve as a screening test to detect articular cartilage injury and it is expected to contribute greatly to the decision on a therapeutic strategy for the management of OA or cartilage injury.

Rheumatology key messages

- Serum keratan sulfate correlates with damage of the articular cartilage.
- It may serve as a screening and monitoring test of the natural course of articular cartilage damage or repair.

Disclosure statement: The authors have declared no conflicts of interest.

References

1 Aroen A, Loken S, Heir S *et al.* Articular cartilage lesions in 993 consecutive knee arthroscopies. Am J Sports Med 2004;32:211–5.
2 Curl WW, Krome J, Gordon ES, Rushing J, Smith BP, Poehling GG. Cartilage injuries: a review of 31,516 knee arthroscopies. Arthroscopy 1997;13:456–60.
3 Hjelle K, Solheim E, Strand T, Muri R, Brittberg M. Articular cartilage defects in 1,000 knee arthroscopies. Arthroscopy 2002;18:730–4.
4 Messner K, Maletius W. The long-term prognosis for severe damage to weight-bearing cartilage in the knee: a 14-year clinical and radiographic follow-up in 28 young athletes. Acta Orthop Scand 1996;67:165–8.
5 Shelbourne KD, Jari S, Gray T. Outcome of untreated traumatic articular cartilage defects of the knee: a natural history study. J Bone Joint Surg Am 2003;85–A (Suppl 2):8–16.
6 Thonar EJ, Lenz ME, Klintworth GK *et al.* Quantification of keratan sulfate in blood as a marker of cartilage catabolism. Arthritis Rheum 1985;28:1367–76.
7 Campion GV, McCrae F, Schnitzer TJ, Lenz ME, Dieppe PA, Thonar EJ. Levels of keratan sulfate in the serum and synovial fluid of patients with osteoarthritis of the knee. Arthritis Rheum 1991;34:1254–9.
8 Belcher C, Yaqub R, Fawthrop F, Bayliss M, Doherty M. Synovial fluid chondroitin and keratan sulphate epitopes, glycosaminoglycans, and hyaluronan in arthritic and normal knees. Ann Rheum Dis 1997;56:299–307.
9 Mundermann A, Dyrby CO, Andriacchi TP, King KB. Serum concentration of cartilage oligomeric matrix protein (COMP) is sensitive to physiological cyclic loading in healthy adults. Osteoarthr Cartilage 2005;13:34–8.
10 Bruyere O, Collette J, Kothari M *et al.* Osteoarthritis, magnetic resonance imaging, and biochemical markers: a one year prospective study. Ann Rheum Dis 2006;65:1050–4.
11 Mazzuca SA, Poole AR, Brandt KD *et al.* Associations between joint space narrowing and molecular markers of collagen and proteoglycan turnover in patients with knee osteoarthritis. J Rheumatol 2006;33:1147–51.
12 Okumura M, Tagami M, Fujinaga T. Measurement of serum and synovial fluid keratan sulphate and antibody to collagen type II in equine osteoarthritis. J Vet Med A 1998;45:513–6.
13 Tomatsu S, Okamura K, Maeda H *et al.* Keratan sulphate levels in mucopolysaccharidoses and mucolipidoses. J Inherit Metab Dis 2005;28:187–202.

14 Kellgren JH, Lawrence JS. Radiological assessment of osteo-arthrosis. Ann Rheum Dis 1957;16:494–502.
15 Ayral X, Altman RD. Arthroscopic evaluation of knee articular cartilage. In: Brandt KD, Doherty M, Lohmander LS, eds. Osteoarthritis. Oxford: Oxford University Press, 1998;494–505.
16 Shinmei M, Miyauchi S, Machida A, Miyazaki K. Quantitation of chondroitin 4-sulfate and chondroitin 6-sulfate in pathologic joint fluid. Arthritis Rheum 1992;35:1304–8.
17 Uesaka S, Nakayama Y, Shirai Y, Yoshihara K. Serum and synovial fluid levels of chondroitin sulfate in patients with osteoarthritis of the knee joint. J Nippon Med Sch 2001;68:165–70.
18 Salisbury C, Sharif M. Relations between synovial fluid and serum concentrations of osteocalcin and other markers of joint tissue turnover in the knee joint compared with peripheral blood. Ann Rheum Dis 1997;56:558–61.
19 Gernero P, Pipermo M, Gineyts E, Christgau S, Delmas PD, Vignon E. Cross sectional evaluation of biochemical markers of bone, cartilage, and synovial tissue metabolism in patients with knee osteoarthritis: relations with disease activity and joint damage. Ann Rheum Dis 2001;60:619–26.
20 Budsberg SC, Lenz ME, Thonar EJ. Serum and synovial fluid concentrations of keratan sulfate and hyaluronan in dogs with induced stifle joint osteoarthritis following cranial cruciate ligament transection. Am J Vet Res 2006;67:429–32.

J Artif Organs (2007) 10:22–28
DOI 10.1007/s10047-006-0363-y

ORIGINAL ARTICLE

Masato Tamai, PhD · Kazuo Isama
Ryusuke Nakaoka, PhD · Toshie Tsuchiya, PhD

Synthesis of a novel β-tricalcium phosphate/hydroxyapatite biphasic calcium phosphate containing niobium ions and evaluation of its osteogenic properties

Abstract To promote the osteogenic properties of osteoblasts, we synthesized a hydroxyapatite (HAp) with β-tricalcium phosphate (β-TCP) biphasic calcium phosphate containing Nb ions (NbTCP/HAp). NbTCP/HAp was prepared by annealing precipitates obtained by coprecipitation of an aqueous solution of $Ca(NO_3)_2$ and a mixture of $(NH_4)_2HPO_4$ and aqueous Nb solution. The precipitates can be regarded as a calcium-deficient HAp, the PO_4 sites of which are partly occupied by Nb ions. NbTCP/HAp was successfully synthesized by thermal decomposition of the precipitates. NbTCP/HAp enhanced the calcification of normal human osteoblasts (NHOst), and the amount of calcified tissue increased in proportion to the Nb ion concentration in the NbTCP/HAp. The alkaline phosphatase (ALP) activity of NHOst was also enhanced by NbTCP/HAp. Because Nb ions significantly enhance the ALP activity of NHOst, calcification by NbTCP/HAp is considered to be due to enhancement of ALP activity induced by Nb ions dissolved from NbTCP/HAp. These results indicate that NbTCP/HAp can be an effective bone repair material.

Key words Tissue engineering · Bone · Osteoblasts · Calcium phosphate · Nb ions

Introduction

Bone tissue engineering offers a promising alternative strategy for healing severe bone injuries by utilizing the body's natural biological response to tissue damage in conjunction with engineering principles. Osteogenic cells, growth factors, and biomaterial scaffolds form the foundation of the many bone tissue engineering strategies employed to achieve regeneration of damaged bone tissue. An ideal biomaterial scaffold will provide mechanical support to an injured site and also enhance osteogenic differentiation to encourage bone growth.[1] To develop biomaterial scaffolds with optimal performance, understanding the interactions between osteoblasts and scaffolds is extremely important.

Hydroxyapatite [HAp, $Ca_{10}(PO_4)_6(OH)_2$] and related calcium phosphate ceramics, e.g., β-tricalcium phosphate [β-TCP, β-$Ca_3(PO_4)_2$], have good biocompatibility with bone tissue because their chemical compositions are very similar to the mineral phase of human bone. It is well known that these calcium phosphate ceramics can be biologically bonded to natural bone. In fact, it has been reported that porous materials composed of HAp, β-TCP, or β-TCP/HAp biphasic calcium phosphate are useful for bone tissue regeneration because of their osteoconductivity.[2–6] It has also been reported that β-TCP/HAp biphasic calcium phosphate shows better osteoconductivity than HAp or β-TCP alone.[7,8] Therefore, this material has been actively studied for use as a scaffold for bone tissue regeneration.

In a previous study, Nb ions were reported to lower cytotoxicity[9] (IC_{50} of Nb ions for L929 fibroblasts is 3.63×10^3), and we reported that Nb ions significantly promoted the calcification of normal human osteoblasts (NHOst).[10] Furthermore, we succeeded in synthesizing a hydroxyapatite containing Nb ions (NbHAp) and showed that NbHAp has the potential to promote alkaline phosphatase (ALP) activity, an important factor in the generation of new bone, in NHOst.[11] In this study, to further promote the cell activity of osteoblasts, we synthesized β-TCP/HAp biphasic calcium phosphate containing Nb ions and investigated interactions between β-TCP/HAp biphasic calcium phosphate and NHOst in vitro.

Materials and methods

Synthesis and characterization of β-TCP/HAp biphasic calcium phosphate containing Nb ions

Reagent grade $Ca(NO_3)_2$, $(NH_4)_2HPO_4$, and $NbCl_5$ (Wako, Osaka, Japan) were used without purification. NbTCP/HAp

Received: May 26, 2006 / Accepted: September 28, 2006

M. Tamai · K. Isama · R. Nakaoka · T. Tsuchiya (✉)
Division of Medical Devices, National Institute of Health Sciences,
1-18-1 Kamiyoga, Setagaya-ku, Tokyo 158-8501, Japan
Tel. +81-3-3700-4842; Fax +81-3-3707-6950
e-mail: tsuchiya@nihs.go.jp

samples were prepared by annealing precipitates obtained from coprecipitation of an aqueous solution of $Ca(NO_3)_2$ with a mixture of $(NH_4)_2HPO_4$ and an aqueous solution of Nb as described below. $Ca(NO_3)_2$ and $(NH_4)_2HPO_4$ were completely dissolved in distilled water. The aqueous Nb solution was prepared by mixing distilled water and $NbCl_5$ dissolved in 5% hydroxyacetone and 5% 2-aminoethanol.[12] A 0.2 M $(NH_4)_2HPO_4$ aqueous solution was combined with 0.01 M $NbCl_5$ and stirred with a magnetic bar at Nb/(Nb + P) molar ratios of 0.0000, 0.0167, or 0.1667. The pH of the mixture was adjusted to 10 using 1 N NaOH throughout the reaction, and 0.2 M $Ca(NO_3)_2$ was slowly dropped into the mixture (20 ml/min). The amount of 0.2 M $Ca(NO_3)_2$ solution was adjusted to a Ca/(Nb + P) molar ratio of 1.6 in order to synthesize β-TCP/HAp biphasic calcium phosphate, followed by stirring the suspension for 24 h at room temperature. The precipitates were centrifuged at 3600 rpm for 5 min and washed with distilled water. The resulting precipitates of Nb/(Nb + P) with molar ratios of 0.0000, 0.0167, and 0.1667 were named NbHAp-0, NbHAp-I, and NbHAp-II, respectively. These precipitates were then annealed at 800°C for 2 h (temperature increase: 5°C/min) and named NbTCP/HAp-0, NbTCP/HAp-I, and NbTCP/HAp-II, respectively. The NbTCP/HAp samples obtained were characterized by X-ray diffraction analysis (XRD, Rint2000, Rigaku, Tokyo, Japan) with Cu K_α radiation (40 kV, 50 mA). The XRD profiles of 2θ angles between 20° and 60° with a step interval of 0.01° were collected at a scanning rate of 4°/min. Also, measurement of the lattice parameter was carried out using the 211, 112, and 300 planes of HAp, and data for the lattice parameter were collected with a scan rate of 0.025°/min. The observed interplanar spacing was corrected using elemental Si as a standard material.

Concentrations of Ca, P, and Nb ions in the precipitate were estimated by inductively coupled plasma analysis (ICP, HP4500, Hewlett-Packard, CA, USA) after the precipitate was dissolved in HNO_3 solution. Microstructural evaluation of the precipitates was performed by scanning electron microscopy (SEM, JSM-5800LV, JEOL, Tokyo, Japan; acceleration voltage: 25 kV) and energy-dispersive X-ray spectroscopy (EDX) (LV5800, JEOL).

Osteogenic effects of NbTCP/HAp

NbTCP/HAp pellets were fabricated to investigate their effects on the osteogenic function of osteoblasts. In total, 100 mg of powdered NbTCP/HAp was put into a stainless steel mold and uniaxially pressed at 30 MPa for 1 min to form a pellet 0.5 mm in thickness and 12 mm in diameter. The pellets were sintered at 800°C for 2 h (temperature increase: 5°C/min).

NHOst were purchased from BioWhittaker (Walkersville, MD, USA) and maintained in d-minimumessential medium (αMEM) (Gibco, Grand Island, NY, USA) containing 10% fetal calf serum (FCS, Kokusai Sinyakyu, Tokyo, Japan) in incubators at 37°C in a humid atmosphere with 5% CO_2. All assays were performed using αMEM containing 10% FCS supplemented with 10 mM β-glycerophosphate.

Cells were seeded on the pellets as described below. Each NbTCP/HAp pellet was immersed in 1 ml culture medium in a well of a 24-well cell culture plate (Corning, Corning, NY, USA) and incubated at 37°C for 24 h. After discarding the medium, 300 μl of new culture medium was put into each well, followed by 1 ml of NHOst suspension (4×10^4 cell/ml), and incubation was carried out for 4 h. Finally, the cell-seeded NbTCP/HAp pellet was transferred to a new well of a 24-well plate with 1 ml of the test medium and incubated at 37°C in a humidified atmosphere with 5% CO_2 for 7–14 days.

Extracts from various NbTCP/HAp samples were prepared to investigate their effects on dissolved ions. NbTCP/HAp powder (100 mg/ml) was added to the culture medium (αMEM) containing 10% FCS and immersed at 37°C for 24 h. After changing the medium, the suspensions were stirred by a shaker at 200 rpm for 72 h at 37°C. The suspension was centrifuged at 3600 rpm for 5 min, and the supernatant was collected to use as an extract for an osteogenesis test in vitro. The atomic concentrations of Nb in the extract were measured by ICP.

An NHOst suspension (4×10^4 cells/ml) was added to culture wells and incubated for 4 h. After the NHOst had adhered to the well, the suspension medium was discarded and 1 ml of the extract supplemented with 10 mM β-glycerophosphate was added. The NHOst were incubated at 37°C in a saturated humid atmosphere with 5% CO_2 for 7–14 days.

We also examined the effect of Nb ions on the osteogenesis of NHOst. A solutionn of 0.2 μM $NbCl_5$/αMEM and serial dilutions were prepared. In addition to the experiment using the extracts indicated above, NHOst were cultured in $NbCl_5$/αMEM supplemented with β-glycerophosphate for 7–14 days.

Proliferation of NHOst cells in each experiment was estimated by a TetraColor One assay (Seikagaku, Tokyo, Japan), which incorporates an oxidation–reduction indicator based on detection of metabolic activity. After a 7-day incubation, the culture medium was discarded and 2% TetraColor One/αMEM solution was added to each well and was incubated for 2 h. The absorbance of the supernatant at 450 nm was measured using a μQuant spectrophotometer (Bio-tek, Winooski, VT, USA) to estimate the proliferation of the test cells. After estimating the proliferation, the cells were washed with phosphate-buffered saline [PBS(–)], followed by the addition of 1 ml of 0.1 M glycine buffer (pH 10.5) containing 10 mM $MgCl_2$, 0.1 mM $ZnCl_2$, and 4 mM *p*-nitrophenylphosphate sodium salt. The absorbance of the added buffer at 405 nm after 5 min incubation at room temperature was detected to evaluate the ALP activity of the test cells. After measurement of ALP, the NHOst cultured in the extract were washed with PBS(–) three times and the calcium phosphate deposited by NHOst was estimated. The amount of deposited calcium phosphate dissolved in 0.1 N HCl solution was determined by a Wako Calcium C test kit (Wako), which is based on the *o*-cresolphthalein complex color development method. The NHOst in all assays were stained in 5% Giemsa solution and observed by light microscopy (Nikon, Eclipse TE300, Tokyo, Japan) to confirm